Influence of Solid Solution Hardening on Creep Properties of Single Crystal Nickel-Based Superalloys

Ernst Fleischmann[1], Christian Konrad[1], Johannes Preußner[2], Rainer Völkl[1], Ernst Affeldt[3], Uwe Glatzel[1]

[1] Metals and Alloys, University Bayreuth, Ludwig-Thoma-Str. 36b, 95447 Bayreuth, Germany

[2] Fraunhofer-Institut für Werkstoffmechanik IWM, Wöhlerstr. 11, 79108 Freiburg

[3] MTU Aero Engines GmbH, Dachauer Str. 665, 80995 München, Germany

Keywords: solid solution, single crystal, creep, nickel based superalloys, rhenium

Abstract

Improving the creep resistance of the matrix by alloying with refractory elements is a major strengthening effect in nickel-based superalloy with rhenium as one of the most effective elements. In this work the influence of rhenium on creep properties of single-phase single crystals with varying rhenium content and matrix near composition is investigated. The use of single crystalline material leads to very distinct results which are not deteriorated by grain boundary effects. So the strengthening effect can be solely attributed to the alloying element rhenium and is quantified for the first time. By comparing the creep strength of two matrix compositions with the corresponding single crystal superalloys using the threshold stress concept the potential of creep strengthening of the matrix in two phase single crystal alloys is quantified.

1. Introduction

Nickel-based superalloys are used as high temperature materials in gas turbines since the 1940s. In order to achieve increased efficiency, the turbine entry temperature is raised steadily leading to higher material temperatures. The temperature capabilities of the alloys used increased over the years by improvements in alloy composition and processing route from wrought alloys to cast single crystal alloys. The outstanding mechanical high temperature properties result from the microstructure consisting of cuboidal shaped $L1_2$-ordered γ'-precipitates coherently embedded in fcc nickel-solid-solution matrix [1]. Many investigations concentrate on optimizing the microstructural parameters like γ'-size $d_{\gamma'}$, γ' volume fraction $f_{\gamma'}$ or misfit δ, see for example [2,3]. Modern single crystal nickel-based superalloys often meet the values $d_{\gamma'} = 0.45\ \mu m$, $f_{\gamma'} = 70\%$ and $\delta = -(1\ldots3)\cdot10^{-3}$, which are considered as optimal [4,5], i.e. precipitation strengthening is exploited to its optimum. Thus creep strengthening of the generally soft matrix by alloying with refractory elements is of high interest. One of the most potent solid solution forming elements for improving the creep resistance of the matrix is rhenium [6] which even led to classification of superalloys in generations according to their rhenium content [7]. The first generation contains no rhenium, the second generation has a rhenium content of 3 wt.%, the third generation 6 wt.% rhenium, the fourth and higher generations also contain ruthenium.

Despite the excellent creep properties the development directions in recent times depart from exotic elements like rhenium and ruthenium because they are scarce strategic elements and are subjected to large price fluctuations [8]. Furthermore rhenium and ruthenium tend to promote the formation of brittle phases that form after long time exposure at high temperatures and thereby have detrimental effects on mechanical properties [9] and on oxidation behavior [10]. Currently efforts are undertaken to develop rhenium free alloys with similar or even better properties than rhenium containing alloys.

Therefore it is important to know why a higher rhenium content leads to a better creep resistance and how big this effect is. In this paper we quantify the effect of rhenium as solid solution forming element on the creep resistance of single crystal matrix alloys. To our knowledge there is no observation that makes it possible to quantify the influence of rhenium on creep behavior of single crystalline matrix alloys in open literature. Two single phase alloys with matrix-near compositions and different rhenium content were cast as single crystals and tested under a constant tensile load at a temperature of 980°C. Due to the use of single crystal material no grain boundary effects like grain boundary sliding adulterate the results and grain boundary strengthening elements need not to be used.

The effect of creep strength of the solid solution matrix alloys on creep properties of the corresponding two phase alloys was determined using the threshold stress concept. The results are compared to the experimentally determined creep behavior of the commercial single crystal nickel-based superalloys CMSX-4 and CMSX-3.

2. Materials and Methods

The commercial superalloy CMSX-4 [11] serves as reference in this investigation. The matrix composition and γ′ phase fraction of CMSX-4 and CMSX-3 at different temperatures were assessed using Thermo-Calc [12] with the database TTNi7 [13]. The calculated compositions agree well with measured matrix composition of CMSX-4 [14]. The composition of the matrix as a function of temperature (see fig. 1) shows a significant increase in γ' forming elements such as Al, Ti and Ta with increasing temperature, reflecting the dissolution of γ'.

Small test samples of alloys with the compositions calculated for the CMSX-4 matrix at 900°C and 800°C were molten and investigated using scanning electron microscopy. The 900°C composition shows γ' precipitates at room-temperature while the alloy with the composition at 800°C does not. So the calculated matrix composition of CMSX-4 at 800°C

was chosen as base matrix composition to ensure that the investigated alloys are indeed single phase at the envisaged temperature of 980°C. The base matrix alloy with 9 wt.% rhenium (designated as MSX Re9) and one alloy without Re (MSX Re0) were cast as single crystals. The composition of MSX Re0 is very close to that of the matrix of CMSX-3 [15]. The nominal composition of the matrix alloys is given in table 1. Microstructure of quenched matrix alloys show no γ' phase.

Master alloys were molten from high purity elements (>99.9%) in an arc furnace under 500 mbar argon atmosphere. Subsequent single crystal casting was carried out in a proprietary Bridgman investment casting furnace [16,17] with a temperature gradient of 6 K/mm and a withdrawal rate of 3 mm/min. The single crystal rods had a diameter of 15 mm and a length of 130 mm. Deviations of the cylindrical axis from the <001> crystallographic direction was in all cases < 9°. Matrix alloys were diffusion heat treated for 60 h at 1280°C to get a homogenous distribution of rhenium and tungsten, which strongly segregate to the dendrite core [18]. CMSX-3 and CMSX-4 were standard heat treated with the parameters given in [19,20].

The microstructures of two phase superalloys in heat treated condition and after an interrupted creep test were examined with a scanning electron microscope (1540EsB, Zeiss) using a column-near secondary electron detector. Samples were prepared by silica polishing and shortly etched (2 s) in Mo etchant (100 ml H_2O, 100 ml HCl (37%), 100 ml HNO_3 (65%), 3 g MoO_3). The volume fraction $f_{\gamma'}$ was determined using area fraction measurements from scanning electron micrographs. To get $f_{\gamma'}$ as a function of temperature small samples (5 x 5 x 1.5 mm^3) were heat treated under Ar for 15 h with subsequent quenching in liquid Ga at a temperature of 35°C to prevent further precipitation of γ'. The room temperature misfit was measured using a powder diffractometer (XRD 3000P, Seifert) working in Bragg-Brentano-geometry. The diffractometer is equipped with a Johansson-monochromator in the

primary beam path to get sole Cu-$K_{\alpha 1}$-radiation. The lattice parameters of matrix a_γ and γ' phase $a_{\gamma'}$ were determined by analyzing the (400)-peak. The constrained misfit was calculated by:

$$\delta_C = \frac{2 \cdot (a_{\gamma'} - a_\gamma)}{(a_{\gamma'} + a_\gamma)} \quad (1)$$

Creep specimens (geometry see [21]) were cut out of single-crystal rods by wire electro discharge machining. To remove the recast layer samples were flat ground to a roughness $R_a < 0.2$ µm. The specimens were machined parallel to the axis of the rod so they have the misorientation resulting from the casting process < 9° off <001>. Creep testing was carried out in proprietary creep testing devices [22,23] under vacuum (<10^{-5} mbar) at a temperature of 980°C and stresses of 30, 50 and 75 MPa for the matrix alloys and 170-300 MPa for nickel-based superalloys. For each two phase superalloy one creep test at 980°C and 200 MPa was interrupted at about 1% strain to investigate the microstructural changes during creep.

3. Results

3.1 Microstructure

In the heat treated condition the two phase alloys possess well aligned cuboidal shaped γ' precipitates with a high volume fraction (see fig. 2). The corners of γ' particles in CMSX-3 are rounder than in CMSX-4 which hints to a slightly lower misfit. This is confirmed by the results of the misfit measurement. The measured γ' precipitate size, γ' volume fraction and constrained misfit at room temperature are given in table 2. The room temperature microstructural properties are very close to each other and to the optimal parameters.

Fig. 3 shows the measured and calculated γ' volume fraction as a function of temperature which are within the measurement error in good agreement to each other. The values for CMSX-3 and CMSX-4 are very close to each other up to a temperature of 1050°C.

The microstructure of the samples which were crept at 980°C and 200 MPa to a strain of 1% can be seen in fig. 4. In both alloys a very similar rafted structure has formed.

3.2 Creep tests

Creep behavior of single-crystal matrix alloys with orientation close to <001> at 980°C is shown in fig. 5. As expected the creep resistance strongly increases with rhenium content. By alloying with 9 wt.% Re the time to rupture is increased and the creep rate decreases by a factor of about 20. The minimum creep rates of the single crystal nickel-based superalloys and the corresponding matrix alloys as well as the finite element results can be seen in the Norton plot in fig. 6. For the Norton plot of the matrix alloys the transition creep rate $\dot{\varepsilon}_t$, which is reached after less than 0.2% strain, is taken instead of the minimum creep rate $\dot{\varepsilon}_{min}$ because all matrix alloys show inverse creep behavior. The Norton exponent n of both matrix alloys is 5.5 ± 0.5. Due to precipitate strengthening of the two-phase alloys minimum creep rates are many orders of magnitude lower than the transition creep rate of matrix alloys.

4. Discussion

By comparing the creep resistance of the three superalloys and their corresponding single crystal matrix alloys in fig. 6 the influence of the improved creep resistance of the matrix can be seen qualitatively.

The back stress σ_P according to eq. 2 can be determined using the Lagneborg-Bergman plot [29] shown in fig. 7 a).

According to Lagneborg and Bergman [29] the precipitates exert a back stress σ_P on the dislocations which leads to a modified version of the Norton creep law, where $\dot{\varepsilon}_{min}$ is the minimum creep rate, A is a constant and σ the applied external stress:

$$\dot{\varepsilon}_{min} = A \cdot (\sigma - \sigma_P)^n \qquad (2)$$

The back stress σ_P can be seen in fig. 7 b). For all superalloys σ_P is increasing with increasing applied stress. This is in good agreement with the theory of Lagneborg and Bergman [29] who showed that σ_P is proportional to the applied stress if it is smaller than the stress necessary to circumvent the precipitates by the Orowan-mechanism or to cut the particles. This trend was confirmed by investigations of Schneider et al. [30]. In this intermediate stress region dislocations are climbing over obstacles.

It is well known that the γ′ morphology changes during creep deformation at high temperatures from cubes to rafts [31]. Rafting has a significant influence on creep behavior [32] and is depending on the magnitude of the misfit. In the rafted microstructure the deformation by bypassing the particles is much more difficult, so penetrating and cutting of particles is important [33]. Improvement of creep strength by the rafted γ′ phase is similar when dislocation network at interface is the same which is also depending on the misfit [33]. Measurements show that this is the case in the investigated alloys at room temperature. Misfit values from literature show a good agreement for CMSX-3 ($\delta \approx -3 \cdot 10^{-3}$ [19]) and CMSX-4 ($\delta \approx -2.4 \cdot 10^{-3}$ [27]) at elevated temperatures as well.

To exclude that the difference in creep behavior is a result of a different rafted structure the microstructure of samples crept to a strain of about 1% were investigated (see fig. 4). It can be seen that both alloys show a very similar rafted microstructure.

The results show that the difference in creep strength is a result of the different creep resistance of the matrix phase if the matrix/γ′ microstructure is similar.

The back stresses in CMSX-3 and CMSX-4 at the same applied stress are very similar. This is a result of the very similar microstructures and misfit, which determine the creep strengthening effect of the particles. This also shows that the difference in the minimum creep rates of CMSX-3 and CMSX-4 is a result of the creep behavior of the matrix.

5. Summary

The influence of the solid solution hardening element Re on creep properties of single crystalline alloys with a composition close to the matrix of second generation nickel-based superalloys was analyzed. The creep resistance of the matrix alloys increases by a factor of 20 by increasing the Re-content from 0 wt.% to 9 wt.%. This means by alloying a two phase superalloy with 3 wt.% Re without changing the microstructure the creep properties can be increased by a factor of 20.

At low stresses the impact of a matrix with higher creep resistance on the mechanical properties of two-phase nickel-based superalloys was analysed:

- The microstructure of the investigated two phase alloys is very similar in undeformed as well as crept samples. Both alloys have similar misfits, γ′ volume fractions and γ′ sizes. The microstructure changes during creep deformation to rafts but still is very similar in both alloys.
- A comparison of the creep strength of the two phase superalloys and the corresponding single crystalline matrix alloys in the Norton plot qualitatively shows the impact of higher matrix strength on two phase alloys.
- Using the threshold stress concept the strengthening effect of the particles can be determined. It was shown that for superalloys with similar γ′ microstructure the back stress from the particles is equal. So higher creep strength of the matrix leads to higher creep strength of the two phase superalloy.

Acknowledgements

The authors thank the Bundesministerium für Wirtschaft und Technologie and MTU Aero Engines AG for funding this work within Lufo 4/3 - AP2.3.

References

[1] C.T. Sims, N.S. Stoloff, W.C. Hagel (Eds.): Superalloys II: High Temperature Materials for Aerospace and Industrial Power, second. ed., WileyBlackwell, New York, 1987.

[2] T. Khan, in: W. Betz, R. Brunetaud, D. Coutsouradis, H. Fischmeister, T.B. Gibbons, I. Kvernes, Y. Lindblom, J.B. Marriot, D.B. Meadowcroft (Eds.): High Temperature Alloys for Gas Turbines and Other Applications, Part I, D. Reidel Publishing Company, Dordrecht, Holland, 1986, pp. 21-50.

[3] M.V. Nathal: Metall. Trans. A, 1987, vol. 18A, pp. 1961-1970.

[4] T. Murakumo, T. Kobayashi, Y. Koizumi, H. Harada: Acta Mater., 2004, vol. 52, pp. 3737-3744.

[5] K. Harris, G.L. Erickson, S.L. Sikkenga, W.D. Brentnall, J.M. Aurrecoechea, K.G. Kubarych: J. Mater. Eng. Perform., 1993, vol. 2, pp. 481-487.

[6] A.K. Jena, M.C. Chaturvedi: Review - The Role of Alloying Elements in the Design of Nickel-base Superalloys, Journal of Materials Science 19 (1984) 3121-3139.

[7] A.D. Cetel, D.N. Duhl, in: S. Reichman, D.N. Duhl, G. Maurer, S. Antolovich, C. Lund (Eds.): Superalloys 1988, TMS, Warrendale, 1988, pp. 235-244.

[8] P.J. Fink, J.L. Miller, D.G. Konitzer: JOM, 2010, vol. 62, pp. 55-57.

[9] C.M.F. Rae, R.C. Reed: Acta mater., 2001, vol. 49, pp. 4113-4125.

[10] K. Kawagishi, H. Harada, A. Sato, A. Sato, T. Kobayashi: JOM, 2006, vol. 58, pp. 43-46.

[11] K. Harris, G.L. Erickson: U.S. Patent 4,643,782, 1987.

[12] B. Sundman, B. Jansson, J.-O. Andersson: CALPHAD, 1985, vol. 9, pp. 153-190.

[13] N. Saunders, M. Fahrmann, C.J. Small, in: T.M. Pollock, R.D. Kissinger, R.R. Bowman, K.A. Green, M. McLean, S. Olson, J.J. Schirra (Eds.): Superalloys 2000, TMS, Warrendale, 2000, pp. 803-811.

[14] N. Wanderka, U. Glatzel: Mater. Sci. Eng. A, 1995, vol. 203A, pp. 69-74.

[15] K. Harris, G.L. Erickson, R.E. Schwer, in: M. Gell, C.S. Kortovich, R.H. Bricknell, W.B. Kent, and J.F. Radavich (Eds.): Superalloys 1984, TMS, Warrendale, 1984, pp. 221-230.

[16] C.H. Konrad, M. Brunner, K. Kyrgyzbaev, R. Völkl, U. Glatzel: J. Mater. Process. Technol., 2011, vol. 211, pp. 181-186.

[17] M. Bensch, E. Fleischmann, C. Konrad, R. Völkl, C.M.F. Rae, U. Glatzel, in: E.S. Huron, R.C. Reed, M.C. Hardy, M.J. Mills, R.E. Montero, P.D. Portella, J. Telesman (Eds.): Superalloys 2012, TMS, Warrendale, 2012, pp. 387-394.

[18] C. Schulze, M. Feller-Kniepmeier: Mater. Sci. Eng. A, 2000, vol. 281A, pp. 204-212.

[19] T.M. Pollock, A.S. Argon: Acta Metall. Mater., 1992, vol. 40, pp. 1-30.

[20] B.C. Wilson, J.A. Hickman, G.E. Fuchs: JOM, 2003, vol. 55, pp. 35-40.

[21] M. Brunner, M. Bensch, R. Völkl, E. Affeldt, U. Glatzel: Mater. Sci. Eng. A, 2012, 550A, pp. 254-262.

[22] R. Völkl, D. Freund, B. Fischer: J. Test. Eval., 2003, vol. 31, pp. 35-43.

[23] R. Völkl, B. Fischer: Exp. Mech., 2004, vol. 44(2), pp. 121-128.

[24] J. Preußner, Y. Rudnik, R. Völkl, U. Glatzel: Int. J. Mater. Res., 2005, vol. 96, pp. 596-601.

[25] J. Preußner, Y. Rudnik, H. Brehm, R. Völkl, U. Glatzel: Int. J. Plast., 2009, vol. 25, pp. 973-994.

[26] L. Müller, U. Glatzel, M. Feller-Kniepmeier: Acta Metall. Mater., 1993, vol. 41, pp. 3401-3411.

[27] D. Siebörger, H. Knake, U. Glatzel: Mater. Sci. Eng. A, 2001, vol. 298A, pp. 26-33.

[28] U. Glatzel, M. Feller-Kniepmeier: Scr. Mater., 1989, vol. 23, pp. 1839-1844.

[29] R. Lagneborg, B. Bergman: Met. Sci., 1976, vol. 10, pp. 20-28.

[30] W. Schneider, J. Hammer, H. Mughrabi, in: S.D. Antolovich, R.A. MacKay, D.L. Anton, T. Khan, R.D. Kissinger, D.L. Klarstrom (Eds.): Superalloys 1992, TMS, Warrendale, 1992, pp. 589-598.

[31] M.V. Nathal, R.A. MacKay: Mater. Sci. Eng., 1987, vol. 85, pp. 127-138.

[32] P. Caron, T. Khan: Mater. Sci. Eng., 1983, vol. 61, pp. 173-184.

[33] J.X. Zhang, J.C. Wang, H. Harada, Y. Koizumi: Acta Mater., 2005, vol. 53, pp. 4623-4633.

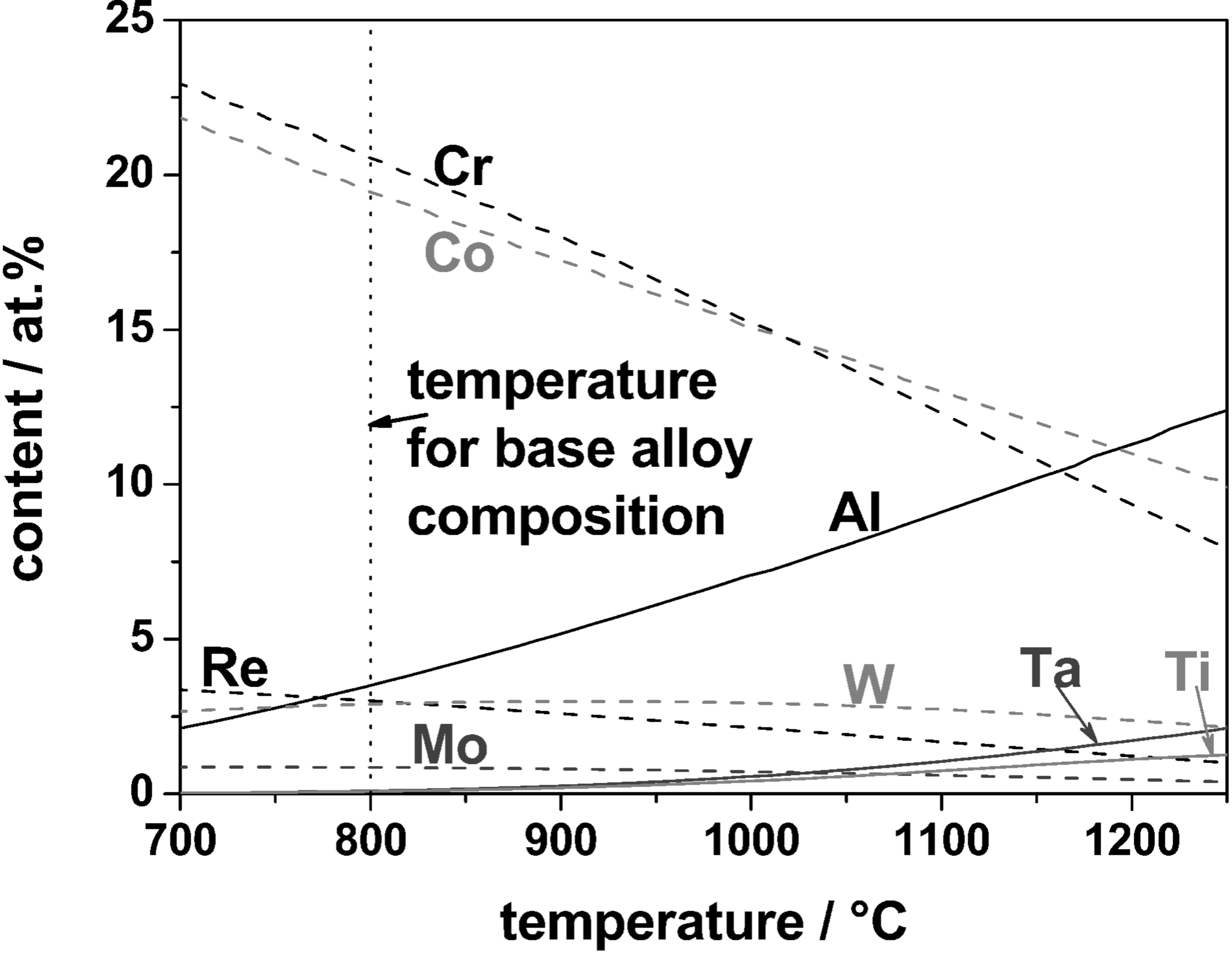

Figure 1: Matrix composition of the alloy CMSX-4 calculated with Thermo-Calc [11] as function of temperature.

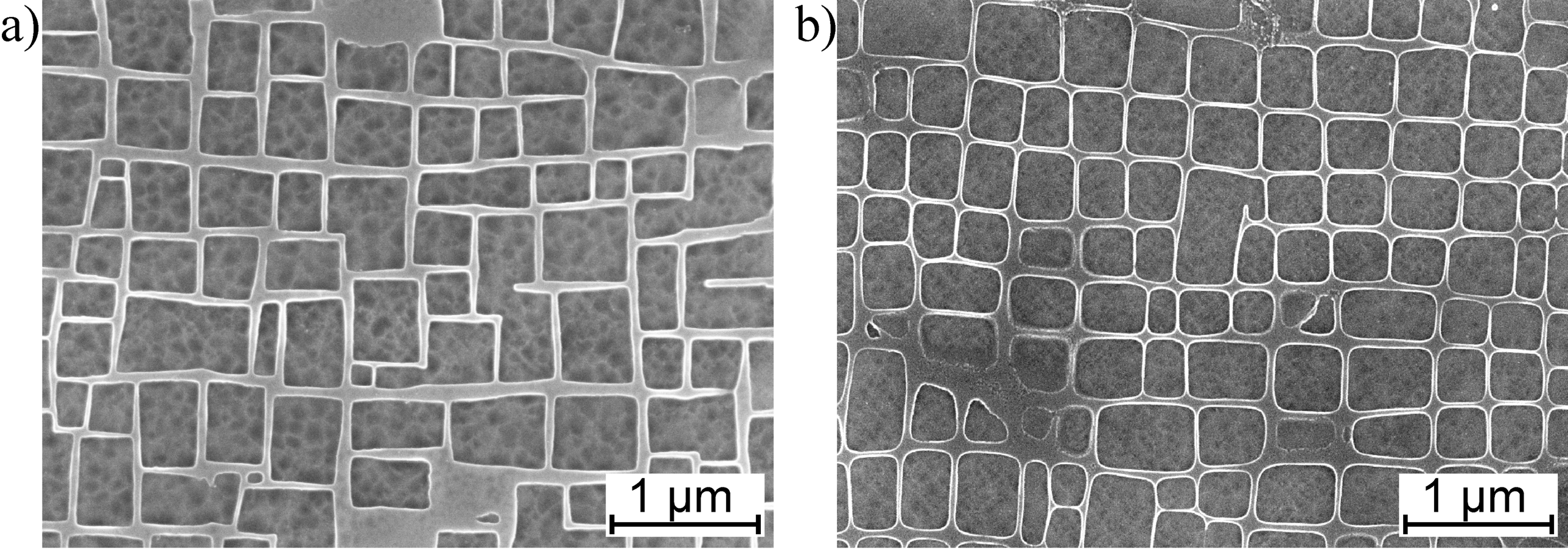

Figure 2: Microstructure of a) CMSX-4 and b) CMSX-3 in heat treated condition. Both alloys show a similar microstructure with cubic shaped γ' particles with a high volume fraction

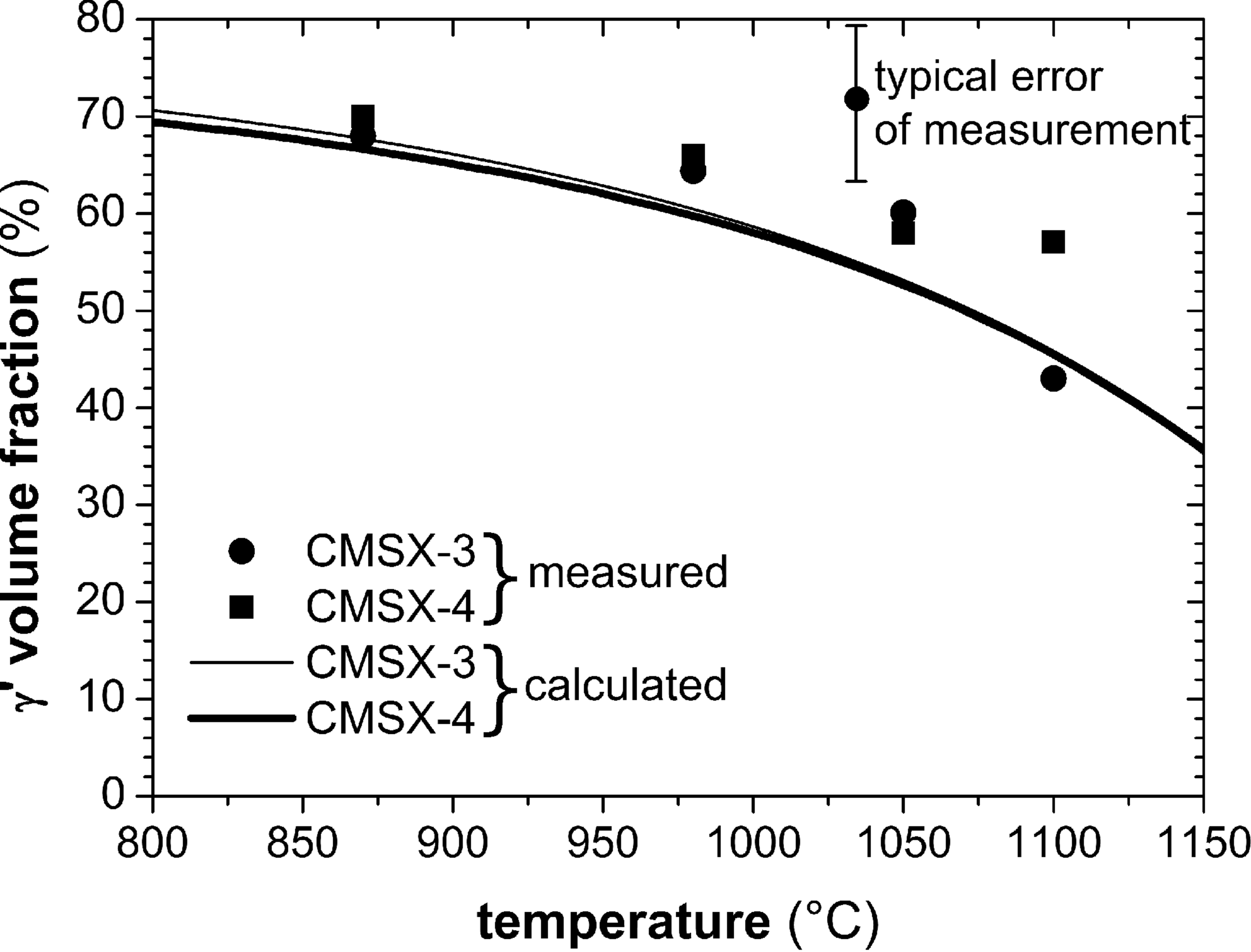

Figure 3: Measured as well as calculated γ' volume fraction as function of temperature.

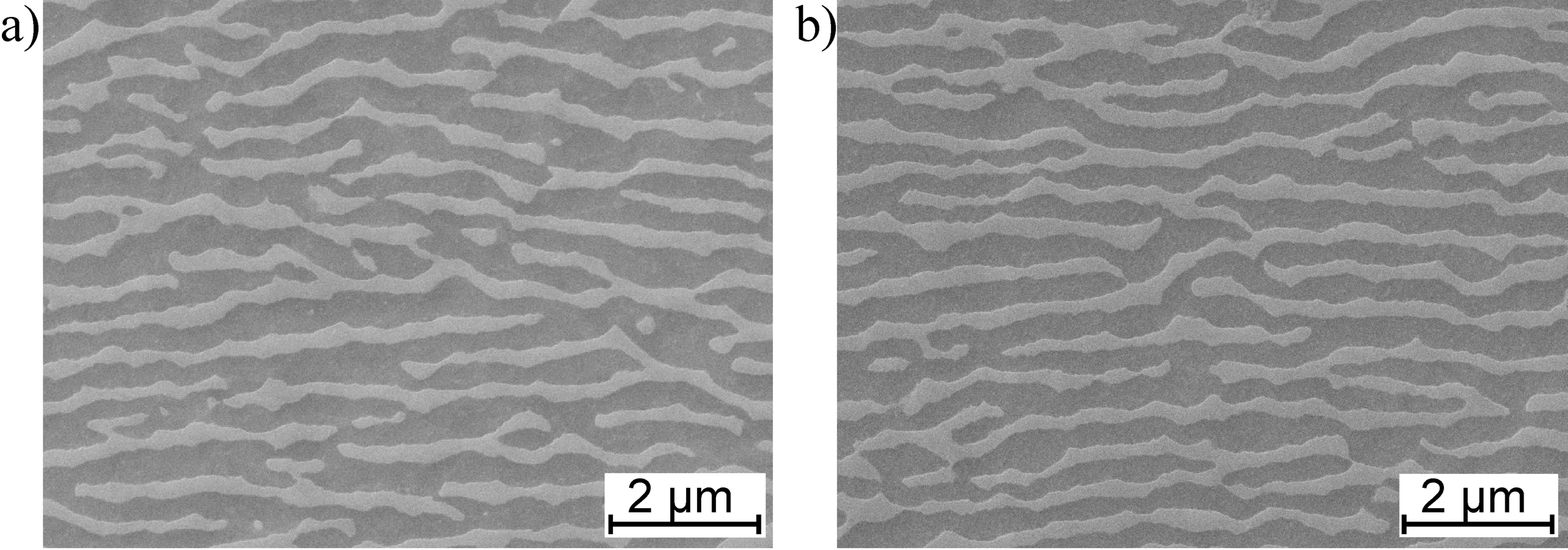

Figure 4: Microstructure of a) CMSX-4 and b) CMSX-3 after creep to 1% strain at 980°C and 200 MPa. Both alloys show a very similar rafted microstructure.

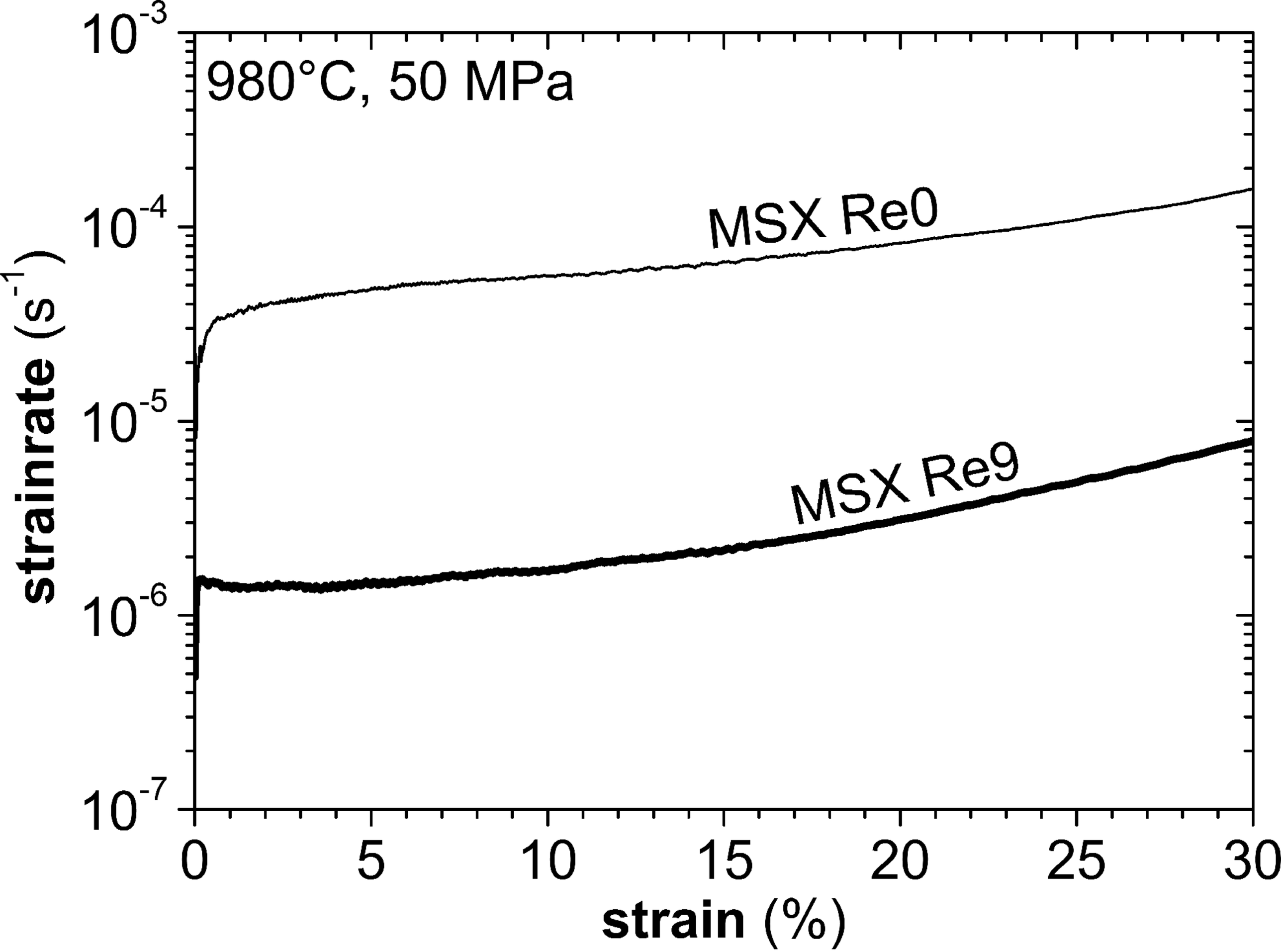

Figure 5: Creep curves of single crystal (001)-oriented matrix alloys with different rhenium content at 980°C and 50 MPa.

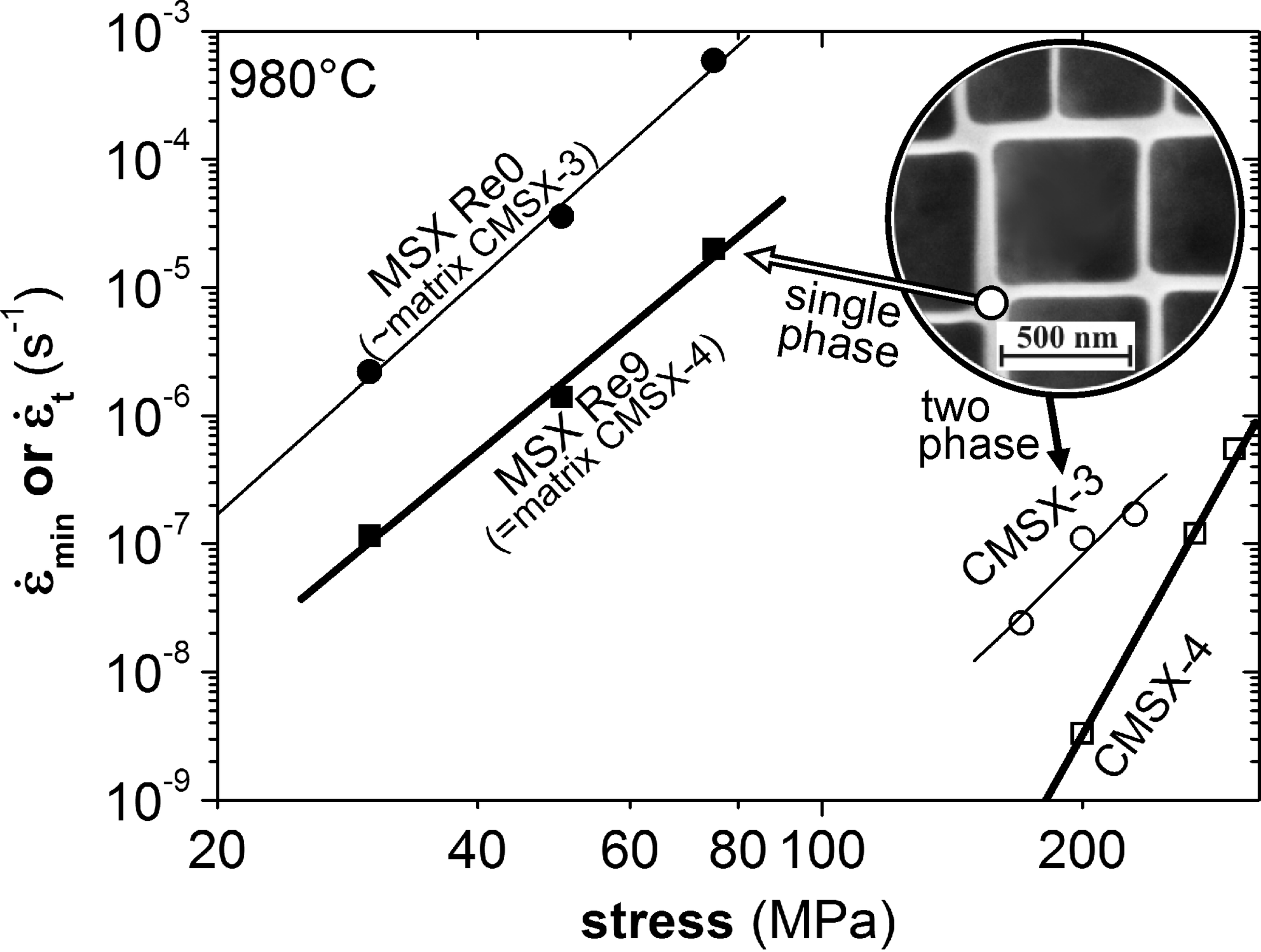

Figure 6: Norton plot showing creep rates of single crystal matrix alloys and corresponding single crystal nickel-based superalloys at 980°C. Thickness of lines indicates rhenium content

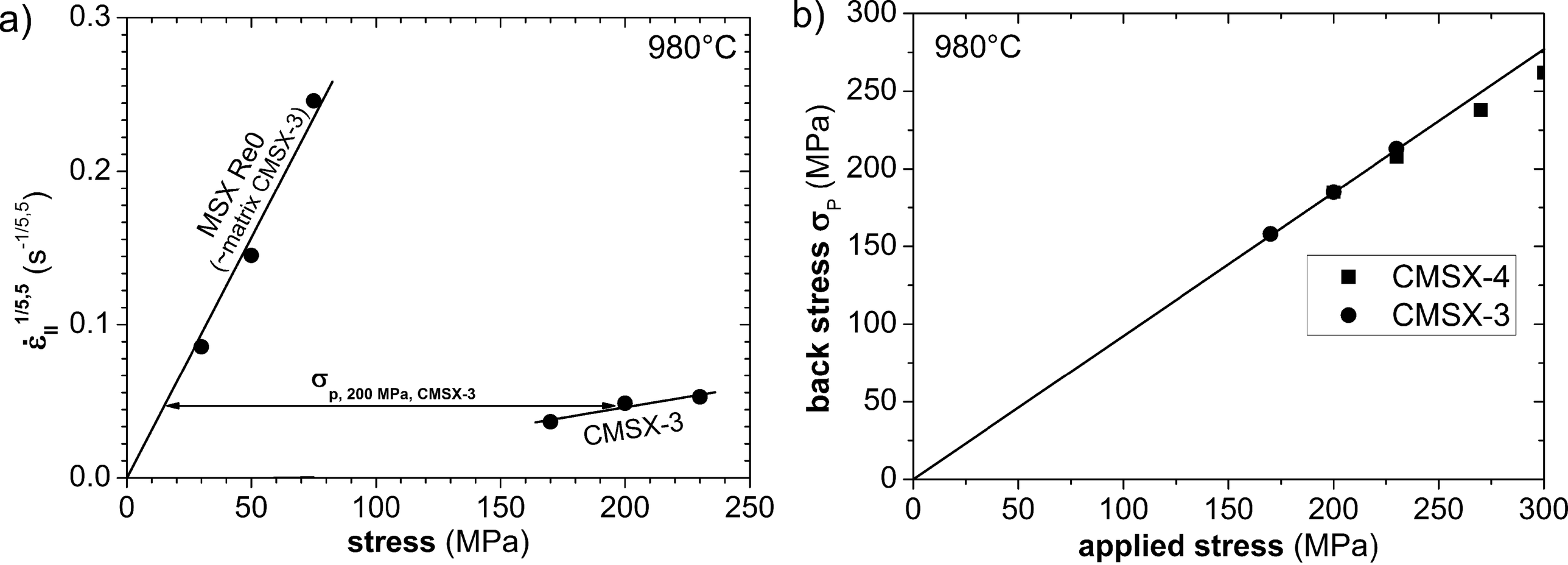

Figure 7: a) Lagneborg-Bergman plot after [28] of CMSX-3 and the corresponding matrix alloy. The arrow indicates the back stress σP at 200 MPa. b) Back stress versus applied stress determined from extrapolated creep data in the Lagneborg-Bergman plot. Back stress is very similar for both alloys and increases with increasing applied stress.

Table 1: Nominal alloy compositions in wt.%. Matrix composition of CMSX-3 and CMSX-4 (according to Thermo-Calc) just listed in order to compare, they were not further tested.

alloy	concentration in wt.%								
	Al	Co	Cr	Mo	Re	Ta	Ti	W	Ni
MSX Re0	1.4	19.8	18.4	1.4	-	0.2	0.1	9.1	49.6
matrix of CMSX-3	1.5	9.1	20.4	1.1	-	0.4	0.1	10.4	57.0
MSX Re9	1.4	18.0	16.7	1.3	9.0	0.2	0.1	8.3	45.0
matrix of CMSX-4	1.4	18.0	16.7	1.3	8.8	0.3	0.1	8.3	45.1

Table 2: Measured γ' precipitate size $d_{\gamma'}$, γ' volume fraction $f_{\gamma'}$ and constrained misfit $\delta_{c,RT}$ at RT of the single crystal nickel-based superalloys CMSX-3 and CMSX-4.

Microstructural properties	Alloy		Ideal value [**Error!**
	CMSX-3	CMSX-4	
$d_{\gamma'}$ (nm)	410 ± 30	470 ± 50	450
$f_{\gamma'}$ (%)	68 ± 5	70 ± 3	70
$\delta_{c,RT}$ (10^{-3})	-1,2	-1,5	-(1…5)